J|A|C|S ARTICLES

Published on Web 02/04/2009

Hybrid Materials and Periodic Mesoporous Organosilicas Containing Covalently Bonded Organic Anion and Cation Featuring MCM-41 and SBA-15 Structure

Abdelkrim El Kadib,[†] Peter Hesemann,*[,‡] Karine Molvinger,[†] Jérôme Brandner,[‡] Christine Biolley,[†] Philippe Gaveau,[†,‡] Joël J. E. Moreau,[‡] and Daniel Brunel*[,†]

Laboratoire MACS, and Laboratoire AM2N, Institut Charles Gerhardt de Montpellier, UMR 5253-CNRS-UM2-ENSCM-UM1, Ecole Nationale Supérieure de Chimie, 8, rue de l'Ecole Normale, 34296 Montpellier Cedex 5, France

Received September 29, 2008; E-mail: daniel.brunel@enscm.fr; peter.hesemann@enscm.fr

Abstract: We report the synthesis of a new trialkoxysilylated ionic liquid based on disilylated guanidinium and monosilylated sulfonimide species. This compound allowed the successful preparation of new periodic mesoporous organosilicas containing covalently anchored ion-pair through both organo-cationic and organo-anionic moieties which have never been reported up to now. Two classes of hybrid materials containing guanidinium−sulfonimide ion-pairs (IPs) have been synthesized. The first type of material was prepared by grafting the silylated IP onto both MCM-41-type and SBA-15-type silicas according to a surface sol−gel polymerization. The second class was synthesized following a one-pot sol−gel procedure using silylated IP and tetraethoxysilane as framework precursors. These latter materials correspond to so-called periodic mesoporous organosilicas (PMOs) and gave "organo-ionically" modified MCM-41 and SBA-15 related solids. The materials were characterized by a series of techniques including XRD, nitrogen sorption, solid-state NMR, FTIR, transmission electronic microscopy, and elemental analysis. The highest structural regularity in terms of pore size distribution and channel size homogeneity was observed for IP-PMOs possessing SBA-15-type architecture due to an enhanced trialkoxysilylated IP precursor/surfactant interaction. Solvatochromic experiments with Reichardt's dye showed good accessibility of the silica-supported ion-pair and suggested the formation of monophasic materials.

1. Introduction

Salts with melting points lower than room temperature have been known for nearly one century, since Walden reported the physical properties of ethylammonium nitrate in 1914.[1] Much later, dialkyimidazolium chloroaluminates were particularly considered in the 1980s due to their electrochemical and acidic properties.[2] The so-called ionic liquid (IL) systems were greeted as a major breakthrough in chemistry science only since the discovery of hydrolytically stable systems in the early 1990s.[3] The versatility of these compounds has its root in the possibility to adjust their physical and chemical properties by varying the ionic components of the ILs. These provide a wide variety of cation−anion combinations, which find emergence application in chromatography,[4] as electrolyte, and, more specially, as solvent media for chemical reactions and extractions.[5−7] The field of ILs has been extensively investigated as green solvents or cocatalysts in various reactions such as organic, biologic, and polymerization catalysis and extraction processes using its adjustable miscibility and polarity in addition with its stability and nonvolatility.[8−18] With the introduction of cleaner technologies becoming a major concern, the supporting of reagents and catalysts is being widely studied as a way of generating green processes throughout both industry and academia.[19] Indeed, the immobilization of ILs on inert supports brings many advantages for the system such as easier separation of the active molecules from the reaction media and better shaping. Physisorbed systems were used in synthesis for fine chemicals.[20] Moreover, covalent anchorage of ionic species on solid support was achieved by Hölderich et al.[20,21] and Mehnert et al.[22] for the valorization of aromatics through their alkylation or their hydroformylation. This approach has been furthermore applied to other catalytic reactions for fine chemical production.[23−25]

[†] Laboratoire MACS.
[‡] Laboratoire AM2N.

(1) Walden, P. *Bull. Acad. Imper. Sci. (St. Petersburg)* **1914**, 405.
(2) Wilkes, J. S.; Levisky, J.; Wilson, R.; Hussey, C. *Inorg. Chem.* **1982**, *21*, 1263–1264.
(3) Wilkes, J. S.; Zaworotko, M. J. *J. Chem. Soc., Chem. Commun.* **1992**, 965–967.
(4) Poole, C. F.; Kersten, B. R.; Ho, S. S. J.; Coddens, M. E.; Furton, K. G. *J. Chromatogr.* **1986**, *352*, 407–425.
(5) (a) Chauvin, Y.; Olivier-Bourbigou, H. *CHEMTECH* **1995**, *25*, 26–30. (b) Chauvin, Y.; Mussmann, L.; Olivier-Bourbigou, H. *Angew. Chem., Int. Ed. Engl.* **1995**, *34*, 2698–2700. (c) Chauvin, H.; Olivier, H.; Wyrvalski, C. N.; Simon, L. C.; de Souza, R. F. *J. Catal.* **1997**, *165*, 275–278. (d) Vallée, C.; Chauvin, Y.; Basset, J.-M.; Santini, C. C.; Galland, J.-C. *Adv. Synth. Catal.* **2005**, *347*, 1835–1847.
(6) Seddon, K. R. *J. Chem. Technol. Biotechnol.* **1997**, *68*, 351–356.
(7) Welton, T. *Chem. Rev.* **1999**, *99*, 2071–2083.
(8) Cull, S. G.; Holbrey, J. D.; Vargas-Mora, V.; Seddon, K. R.; Lye, G. J. *Biotechnol. Bioeng.* **2000**, *69*, 227–233.
(9) Sheldon, R. *Chem. Commun.* **2001**, 2399–2407.
(10) Gordon, C. M. *Appl. Catal., A* **2001**, *222*, 101–117.
(11) Swatloski, R. P.; Spear, S. K.; Holbrey, J. D.; Rogers, R. D. *J. Am. Chem. Soc.* **2002**, *124*, 4974–75.

 10.1021/ja807630j CCC: $40.75

Hence, the immobilization of ILs on mineral oxide is currently of great interest not only for their use as catalysts, but also for the envisaged formation of well-structured materials possessing unique chemical surface properties. In this respect, we have already focused on the synthesis of mesoporous silica functionalized with imidazolium species by one-pot hydrolysis polycondensation using monosilylated ionic precursors.[26] Material containing imidazolium-bridged silesquioxane has been already synthesized[27] through the hydrolytic polycondensation of bis-silylated organic moieties[28,29] in the presence of a structure-directing agent as shown by Inagaki et al. to generate the porosity of these so-called periodic mesoporous organosilicas (PMOs).[30,31] As far as the structuring of the PMOs is concerned, to make them more attractive as covalent scaffolding hosts whatever the nature of the organic bridge, extensive efforts were directed to enlarge their porosity.[32,33] Whereas PMOs prepared by structure-directing agents with ionic alkyl ammonium surfactants feature pore diameters restricted to the range between 2 and 5 nm, those of PMOs synthesized with nonionic surfactant in acidic media possess in contrast the largest pores.[34] The synthesis of the latter using the neutral triblock copolymer P123 ($EO_{20}PO_{70}EO_{20}$) takes place according to a $(S^0H^+)(X^-I^+)$ pathway and presents a SBA-15-like structure. It is noteworthy that the degree of order of these materials structured by triblock copolymers could be improved by the addition of inorganic salts such as NaCl to the reaction mixture. Indeed, Guo et al. were able to obtain a highly ordered large-pore ethane-bridged PMO (pore size diameter $D = 6.4$ nm).[35] The specific effect of this salt on the interaction between the positively charged headgroup of the surfactant and the inorganic species prompted us to investigate the synthesis of PMOs possessing ion-pair (IP) in the framework using P123 as a structure-directing agent. For comparison, the functionalization of pure SBA-15 was performed through a surface coating by polysilylated organo-ions-pair to point out the role of the IP−surfactant interaction on the hybrid SBA-15-type material structuration.

However, we have also investigated the design of MCM-41-type materials containing an IP system using CTAB as ionic surfactant agents for the preparation of PMOs-type hybrid material, and the surface coating of MCM-41 silica surface to point out the role of IL/template interaction, depending on the surfactant nature. For this purpose, we have first investigated the synthesis of trialkoxysilyl organo-ions-pair through fixing trialkoxysilane groups on each ionic component. In this respect, guanidinium and *N*-phenylsulfonyl-*N*′-trifluorosulfonylimide have been selected as the two IP components, guanidinium being possibly bis-silylated and sulfonimide being silylated on the phenyl group through an 4-ethyl linker. Second, this precursor has been further used to synthesize meso-structured hybrid materials possessing silica-nanostructured framework and ionic liquid tethered by means of both cation and anion components. PMOs materials were prepared by co-condensation of these trisilylated organoion-pairs with TEOS in the presence of surfactant in parallel with meso-structured silica-containing grafted organo-ion-pair using these precursors by coating of pure mesoporous silica surface for comparison. As the location of the organic ions into the PMOs materials was questionable, we have studied the accessibility to the IP molecules in the PMOs versus grafted mesostructured silicas using an optical probe. Actually, most of the ILs revealed unexpected high solvatochromic polarities based on absorption of probes such as Reichardt's dye (RD), which is the most common negative solvatochromic charge-transfer absorption probe for liquids.[36,37] More recently, RD was also used to probe the surface polarity of solid surface.[38,39] Therefore, we adopted such an approach in this work to control the IP-tethered location on the silica framework by comparing the surface polarity of the IP-tethered surface to that of the homogeneous counterpart.

2. Experimental Section

2.1. General. Unless otherwise specified, all preparation manipulation reactions were performed under argon or nitrogen using standard Schlenk-tube techniques or an inert atmosphere drybox.

(12) (a) Zhao, H.; Xia, S.; Ma, P. *J. Chem. Technol. Biotechnol.* **2005**, *80*, 1089–1096. (b) Zhao, H. *Chem. Eng. Commun.* **2006**, *193*, 1660–1677.
(13) van Rantwijk, F.; Sheldon, R. *Chem. Rev.* **2007**, *107*, 2757–2785.
(14) Weingärtner, H. *Angew. Chem., Int. Ed.* **2007**, *46*, 2–19.
(15) Ranke, J.; Stolte, S.; Störmann, R.; Arning, J.; Jastorff, B. *Chem. Rev.* **2007**, *107*, 2183–2206.
(16) Pârvulescu, V. I.; Hardacre, C. *Chem. Rev.* **2007**, *107*, 2615–2665.
(17) Johnson, K. E.; Pagni, R. M.; Bartmess, J. *Monatsh. Chem.* **2007**, *138*, 1077–1101.
(18) Plechkova, N. V.; Seddon, K. R. *Chem. Soc. Rev.* **2008**, *37*, 123–150.
(19) Clark, J. H.; Macquarrie, D. J. *Chem. Soc. Rev.* **1996**, *25*, 303–310.
(20) (a) Riisager, A.; Fehrmann, R.; Haumann, M.; Wasserscheid, P. *Eur. J. Inorg. Chem.* **2006**, 695–706. (b) Breitenlechner, S.; Fleck, M.; Müller, T. E.; Suppan, A. *J. Mol. Catal. A* **2004**, *214*, 175–179. (c) Jiminez, O.; Müller, T. E.; Sievers, C.; Spirkl, A.; Lercher, J. A. *Chem. Commun.* **2006**, 2974–2976. (d) Mikkola, J. P. T.; Virtanen, P. P.; Kordas, K.; Karhu, H.; Salmi, T. O. *Appl. Catal., A* **2007**, *328*, 68–76. (e) Gu, Y.; Karam, A.; Jérôme, F.; Barrault, J. *Org. Lett.* **2007**, *9*, 3145–3148. (f) Alaerts, L.; Wahlen, J.; Jacobs, P. A.; de Vos, D. E. *Chem. Commun.* **2008**, 1727–1737. (g) Burguete, M. I.; Erythropel, H.; Garcia-Verdugo, E.; Luis, S. V.; Sans, V. *Green Chem.* **2008**, *10*, 401–407.
(21) (a) Valkenberg, M. H.; deCastro, C.; Hölderich, W. F. *Appl. Catal., A* **2001**, *215*, 185–190. (b) Valkenberg, M. H.; Hölderich, W. F. *Green Chem.* **2002**, *4*, 88–93. (c) Kumar, P.; Vermeiren, W.; Dath, J.-P.; Hölderich, W. F. *Appl. Catal., A* **2006**, *304*, 131–141.
(22) (a) Mehnert, C. P.; Cook, R. A.; Dispenziere, N. C.; Afeworki, M. *J. Am. Chem. Soc.* **2002**, *124*, 12932–12933. (b) Mehnert, C. P. *Chem.-Eur. J.* **2005**, *11*, 50–56.
(23) Liu, Y.; Peng, J.; Zhai, S.; Li, J.; Mao, J.; Li, M.; Qui, H.; Lai, G. *Eur. J. Inorg. Chem.* **2006**, 2947–2949.
(24) Lou, L. L.; Yu, K.; Ding, F.; Zhou, W.; Peng, X.; Liu, S. *Tetrahedron Lett.* **2006**, *47*, 6513–6516.
(25) Yan, Y.; Nie, J.; Zhang, Z.; Wang, S. *Appl. Catal., A* **2005**, *295*, 170–176.
(26) (a) Gadenne, B.; Hesemann, P.; Moreau, J. J. E. *Chem. Commun.* **2004**, 1768–1769. (b) Gadenne, B.; Hesemann, P.; Polshettiwar, V.; Moreau, J. J. E. *Eur. J. Inorg. Chem.* **2006**, 3697–3702.
(27) Lee, B.; Im, H.-J.; Luo, H.; Hagaman, E. W.; Dai, S. *Langmuir* **2005**, *21*, 5372–5376.
(28) (a) Shea, K. J.; Kenneth, J.; Loy, D. A.; Webster, O. W. *Chem. Mater.* **1989**, *1*, 572–574. (b) Shea, K. J.; Loy, D. A.; Webster, O. W. *J. Am. Chem. Soc.* **1992**, *114*, 6700–6710.
(29) (a) Corriu, R. J. P.; Moreau, J. J. E.; Thepot, Ph.; Wong Chi Man, M. *Chem. Mater.* **1992**, *4*, 1217–24. (b) Corriu, R. J. P.; Hesemann, P.; Lanneau, G. F. *Chem. Commun.* **1996**, 1845–1846.
(30) (a) Inagaki, S.; Guan, S.; Fukushima, Y.; Ohsuna, T.; Terasaki, O. *J. Am. Chem. Soc.* **1999**, *121*, 9611–9614. (b) Guan, S.; Inagaki, S.; Ohsuna, T.; Terasaki, O. *J. Am. Chem. Soc.* **2000**, *122*, 5660–5661.
(31) (a) Yang, Q.; Kapoor, M. P.; Inagaki, S. *J. Am. Chem. Soc.* **2002**, *124*, 9694–9695. (b) Fujita, S.; Inagaki, S. *Chem. Mater.* **2008**, *20*, 891–90.
(32) Goto, Y.; Inagaki, S. *Chem. Commun.* **2002**, 2410–2411.
(33) Zhu, H.; Jones, D. J.; Zajac, J.; Dutartre, R.; Rhomari, M.; Rozière, J. *Chem. Mater.* **2002**, *14*, 4886–4894.
(34) Hoffmann, F.; Cornelius, M.; Morell, J.; Fröba, M. *Angew. Chem., Int. Ed.* **2006**, *45*, 3216–3251.
(35) Guo, W.; Park, J.-Y.; Oh, M.-O.; Jeong, H.-W.; Cho, W.-J.; Kim, I.; Ha, C.-S. *Chem. Mater.* **2003**, *15*, 2295–2298.
(36) Fletcher, K. A.; Storey, I. A.; Hendricks, A. E.; Pandey, S. *Green Chem.* **2001**, *3*, 210–215.
(37) Reichardt, C. *Solvents and Solvents Effects in Organic Chemistry*, 2nd ed.; Wiley-VCH: Weinheim, Germany/New York, NY, 1990; 3rd ed., 2003.

All reagents purchased from commercial sources were used without further purification unless otherwise specified. In experiments requiring dry free oxygen solvents, THF, toluene, and diethylether were distilled from sodium/benzophenone, DMF was distilled from CaH_2, and CH_2Cl_2 was distilled over P_2O_5 and stored under argon. Elemental analyses were performed by the "Service Central de Microanalyse du CNRS" at Vernaison, France. Nitrogen sorption isotherms at 77 K were obtained with a Micromeritics ASAP 2010 apparatus. Prior to measurement, the samples were degassed under vacuum (0.01 mbar) for 8 h at 250 °C for pure silica materials and at 120 °C for the organosilicas. The surface area (S_{BET}) was determined from BET treatment in the range 0.04−0.3 p/p_0, and assuming a surface coverage of nitrogen molecule estimated to 13.5 Å^2.[40] The mesopore volume and the pore diameter were calculated using the nitrogen volume adsorbed when the capillary condensation is ended and from the BdB model,[41] respectively. Thermogravimetric analyses were performed with a Netzsch TG 209 C apparatus. TEM images were obtained using a JEOL 1200 EX II (120 kV). DRIFT spectra were performed on a Bruker vector 22. DRX were performed on a D8 Advance Bruker AXS (powder diffraction, geometry: Bragg−Brentano). ^{1}H, ^{13}C, ^{19}F, and ^{29}Si NMR spectra in solution were recorded on a Bruker AC 250 MHz or a Bruker Avance 400 MHz spectrometer at room temperature. Deuterated chloroform was used as solvent for liquid NMR experiments, and chemical shifts are reported as δ values in parts per million relative to tetramethylsilane. Solid-state ^{13}C and ^{29}Si MAS NMR experiments were performed on a Varian VNMRS 400 MHz solid spectrometer using a two-channels probe with 7.5 mm ZrO_2 rotors. The ^{29}Si solid NMR spectra were recorded using both CP MAS and one-pulse sequences with samples spinning at 6 kHz. CP MAS was used to get a high signal-to-noise ratio with 5 ms contact time and 5 s recycling delay. For one-pulse experiments, $\pi/6$ pulse and 60 s recycling delay were used to obtain quantitative information on the silane−silanol condensation degree. The ^{13}C CP MAS spectra were obtained using 3 ms contact time, 5 s recycling delay, and 6 kHz spinning rate. DRUV spectra were measured in the 200−800 nm range using $BaSO_4$ as the reference on a Perkin-Elmer Lambda 14 spectrometer equipped with an integrating sphere (Labsphere, North Sutton, USA). Quartz cells (Hellma) of 0.05 mm path length were used. IR data were obtained on a Perkin-Elmer 1000 FT-IR spectrometer. MS-ESI were measured on Water Q-Tof mass spectrometer. SEM images were obtained with a JEOL 6300F microscope.

2.2. Reagents. Karstedt's catalyst (2.1 wt % Pt in xylenes), Aerosil silica 200V, was supplied by Degussa, 3-iodopropyltriethoxysilane, triethylamine, cetylammonium bromide (CTAB), Pluronic P123 (M = 5800 g; viscosity 350 000 cps), tetraethylorthosilicate (TEOS), ethylamine (EA), and bis-*O*,*N*-trimethylsilyltrifluoracetamide were purchased from Aldrich, 2-(4-chlorosulfonylphenyl)ethyltrimethoxysilane was from Fluorochem, and trifluoromethane-sulfonamide was from Alfa Aesar. Syntheses of the parent MCM-41 and SBA-15 type silicas were carried out according to the experimental procedures given in the Supporting Information.

2.3. Synthesis of the Tris-(triethoxy)silylated Guanidinium−Sulfonimide Ion-Pair. 2-Chloro-1,3-dimethylimidazolinium chloride (DMC, **1**) was prepared according to known procedures from 1,3-dimethylimidazolidine-2-one.[42]

Allyl-(1,3-dimethyl-imidazolidin-2-ylidene)-amine (2a). To a solution of freshly prepared 2-chloro-1,3-dimethylimidazolinium chloride (9.15 g; 54 mmol) dissolved in 40 mL of dichloromethane were added 15 mL of triethylamine and finally 4.1 mL (3.12 g; 54 mmol) of allylamine. The resulting reaction mixture was stirred at room temperature and than heated to reflux during 2 h. After being cooled, the reaction mixture was poured into 1 N aqueous hydrochloric acid and extracted with dichloromethane (3 × 50 mL). The volatiles were evaporated, and the resulting solid residue was dissolved in 50 mL of 4 N aqueous NaOH. The resulting solution was extracted with dichloromethane, and the organic phase was dried over Na_2SO_4 and filtered. Finally, the organic solvent was evaporated to give the crude guanidine, which was purified by distillation under reduced pressure (bp ∼70 °C$^{0.01}$) to give the product as a colorless liquid. Yield: 6.70 g; 43.7 mmol (81%). ^{1}H NMR ($CDCl_3$): δ 2.74 (bs, 6H), 3.09 (s, 4H), 3.99 (m, 2H), 4.99 (m, 1H), 5.18−5.23 (m, 1H), 5.92−5.99 (m, 1H). ^{13}C NMR ($CDCl_3$): δ 36.18 (bs), 44.94, 49.32 (bs), 49.55, 113.04, 139.51, 157.52. FT-IR(KBr) ν_{max}/cm^{-1} 3074, 3004, 2936, 2837, 1666, 1638, 1267, 954. HRMS [FAB+] calcd for $C_8H_{16}N_3$ $(M + H)^+$ 154.1344, found 154.1334.

1-(1,3-Dimethyl-imidazolidin-2-ylidene)-3-(triethoxysilyl)-propylamine (2a′). Under argon, 200 μL of Karstedt's catalyst was added dropwise at 0 °C to a solution containing 1 g (6.5 mmol) of allyl-(1,3-dimethyl-imidazolidin-2-ylidene)-amine (**2a**) and 1.30 g (7.9 mmol) of triethoxysilane. The resulting solution was stirred at 0 °C for further 30 min and was finally heated to 60 °C for 30 min. The silylated product was obtained as a colorless liquid after distillation of the crude reaction mixture (bp 134 −136 °C$^{0.1}$). Yield: 1.73 g (84%). ^{1}H NMR ($CDCl_3$): δ 0.59 (m, 2H), 1.10 (t, 9H, J = 7.0 Hz), 1.53 (m, 2H), 2.56 (bs, 3H), 2.75 (bs, 3H), 3.00 (bs, 4H), 3.22 (m, 2H), 3.69 (q, 6H, J = 6.9 Hz). ^{13}C NMR ($CDCl_3$): δ 7.16, 18.27, 23.92, 35.54, 45.82, 49.54, 58.41, 159.05. ^{29}Si NMR ($CDCl_3$): δ −44.92 (s). FT-IR(KBr) ν_{max}/cm^{-1} 2973, 2927, 2882, 1669, 1385, 1265, 1167, 1078, 955. HRMS [FAB+] calcd for $C_{14}H_{32}N_3O_3Si$ $(M + H)^+$ 318.2213, found 318.2221.

***N*-(1,3-Dimethylimidazolidin-2-ylidene)-*N*,*N*-[bis-(3-(triethoxysilyl)-propyl]-1-aminium Iodide (3a).** Under argon, 1 g (3.15 mmol) of 1-(1,3-dimethyl-imidazolidin-2-ylidene)-3-(triethoxysilyl)-propylamine (**2a′**) and 1.70 g (5.1 mmol) of 3-iodopropyltriethoxysilane were mixed and heated to 60 °C overnight. After the mixture was cooled to room temperature, the excess of iodopropyltriethoxysilane was eliminated by distillation to give the guanidinium iodide (**3**) as a viscous brownish oil in quantitative yield. ^{1}H NMR ($CDCl_3$): δ 0.56 (m, 4H), 1.16 (t, 18H, J = 7.0 Hz), 1.66 (m, 4H), 3.05 (s, 6H), 3.25 (m, 4H), 3.76 (q, 6H, J = 7.1 Hz), 3.93 (s, 4H). ^{13}C NMR ($CDCl_3$): δ 6.78, 17.97, 20.07, 36.52, 49.44, 50.87, 58.09, 163.61. ^{29}Si NMR ($CDCl_3$) δ −46.38 (s). FT-IR(KBr) ν_{max}/cm^{-1} 2973, 2927, 2886, 1608, 1569, 1304, 1166, 1079, 957. MS [FAB+] m/z 522 (100). HR-ESI (pos): M (found) = 522.3425; M (calc) = 522.3395.

Triethylammonium 2-[(Trifluoromethanesulfonylimido)-*N*-4-sulfonylphenyl]ethyl-trimethoxysilane (5a). 2-(4-Chlorosulfonylphenyl)ethyltrimethoxysilane **4a** (2 g; 6.71 mmol) was added under argon to a solution of trifluoromethanesulfonamide (1 g; 6.71 mmol) and triethylamine (3.38 g; 33.5 mmol) into 30 mL of methylene dichloride (30 mL). The reaction mixture was stirred and heated at 40 °C overnight. An orange-brown-colored wax was obtained after distillation of the solvent and triethylamine under vacuum. ^{1}H NMR ($CDCl_3$): δ 0.91 (m, 2H), 1.30 (t, 18H, J = 7.4 Hz), 2.69 (m, 2H), 3.08 (q, 12H, J = 7.4 Hz), 3.50 (s, 9H), 7.21 (m, 2H), 7.60 (m, 2H). ^{13}C NMR ($CDCl_3$): δ 7.50, 8.65, 28.59, 46.26, 50.58, 126.70, 127.78, 141.25, 148.42. ^{19}F NMR ($CDCl_3$): δ −78.22 ppm(s). FT-IR(KBr) ν_{max}/cm^{-1} 3474, 2982, 1598, 1475, 1398, 1323, 1187, 1133, 1056, 790. MS [LR-ESI (−)] m/z 436. 1. HR-ESI (neg.): M (found) = 436.0172, M (calc) = 436.0168. ^{19}F NMR chemical shift at −78.11 ppm relative to CF_3COOH with another at −79.24 ppm (relative intensity: <8%) characteristic of $CF_3SO_2NH_2$.

***N*-(1,3-Dimethylimidazolidin-2-ylidene)-*N*,*N*-[bis-(3-(triethoxysilyl)-propyl]-1-aminium 2-[(Trifluoro-methanesulfonylimido)-*N*-4-sulfonylphenyl]ethyl-trimethoxysilane (6a).** A solution of triethylammonium 2-[(trifluoromethanesulfonylimido)-*N*-4-sulfonylphenyl-]ethyltrimethoxysilane (**5a**) in 10 mL of freshly distilled methylene dichloride was added under argon to a solution of (**3a**) *N*-(1,3-dimethylimidazolidin-2-ylidene)-*N*,*N*-[bis-(3-(triethoxysilyl)-

(38) Chronister, C.; Drago, R. S. *J. Am. Chem. Soc.* **1993**, *115*, 4793–4798.
(39) Rottman, C.; Grader, G. S.; Hazan, Y. D.; Avnir, D. *Langmuir* **1996**, *12*, 5505–5508.

propyl]-1-aminium iodide in 10 mL of freshly distilled methylene dichloride. After evaporation of the solvent under vacuum, the as-obtained silylated precursor (**6**) was further used without purification. FT-IR(KBr) ν_{max}/cm^{-1} 2975, 2930, 1608, 1568, 1392, 1325, 1187, 1080, 958, 793. MS [LR ESI (+)]: $M = 522.4$. [LR ESI (−)]: $M = 436.1$.

2.4. Synthesis of the Nonsilylated Ionic Liquid. *N*-(1,3-Dimethylimidazolidin-2-ylidene)-*N*,*N*-[dipropyl]-1-aminium 2-[(Trifluoro-methane-sulfonylimido)-*N*-4-sulfonyltoluene (6b). The preparation of the nonsilylated counterpart (**6b**) of the silylated ion-pair (**6a**) was carried out using the same synthetic route except for the use of 1-aminopropane instead of allylamine as reagent for the preparation of (1,3-dimethyl-imidazolidin-2-ylidene)propylamine (**2b**), the use of 1-iodopropane in place of the 3-iodopropyltriethoxysilane for the preparation of *N*-(1,3-dimethylimidazolidin-2-ylidene)-*N*,*N*-(bis-propyl-1-aminium iodide (**3b**), and the use of *p*-toluenesulfonyl chloride (**4b**) in place of 2-(4-chlorosulfonylphenyl)ethyltrimethoxysilane (**4a**) for the preparation of triethylammonium 2-[(trifluoromethanesulfonylimido)-*N*-4-toluenesulfonyl] (**5b**). Moreover, the purification of crude product was achieved by aqueous workup using methylene chloride as organic solvent. The ionic liquid **6b** was recovered after evaporation of the solvent under vacuum. Yield: 97%. ^{1}H NMR ($CDCl_3$): δ ppm 0.85 (t, 6H, J = 7.3 Hz), 1.56 (m, 4H), 2.30 (s, 3H), 2.97 (s, 6H), 3.16 (broad t, 4H, J = 7.3 Hz), 3.83 (s, 4H), 7.13 (m, 2H), 7.67 (m, 2H). ^{13}C NMR (neat): δ ppm 10.35, 20.39, 20.60, 35.52, 48.61, 50.33, 120.56, 126.26, 128.81, 141.42, 142.93, 163.72. ^{19}F NMR ($CDCl_3$): δ −78.39 ppm(s). FT-IR (KBr) ν_{max}/cm^{-1} 2969, 2879, 1609, 1568, 1324, 1191, 1092, 1055. MS [LR-ESI(−)]: $M = 301.6$. [LR-ESI(+)]: $M = 198.3$.

2.5. Grafting of Mesoporous Silicas (IP-G-MCM-41/IP-G-SBA-15) with Trisilylated Guanidinium−Sulfonimide Ionic Liquid (6a). Activated (180 °C under vacuum; 12 h) silicas (MCM-41, 1.8 g; SBA-15, 2.25 g) were suspended in 30 mL of dry toluene. After addition of 3 mmol of **6a** (corresponding to 9 mmol of trialkoxysilane groups) in both reaction mixtures, these two suspensions were stirred at room temperature for an additional 1 h. Next, 250 μL of water (1.5 equiv versus trialkoxysilane), of 135 mg (0.05 equiv) of *p*-toluenesulfonic acid and 25 mg (0.05 equiv) of NH_4F was poured in each reactor, which were left at room temperature for 1 h, then heated at 60 °C for 6 h, and then heated at 120 °C for 1 h (Dean−Stark). The powders were collected by filtration and successively washed with toluene, methanol, methanol: water (1:1), methanol, and diethyl-ether. They were then extracted with a Soxhlet apparatus (CH_2Cl_2−EtOH) and dried in air at 80 °C.

2.6. Synthesis of PMOs-type Containing Tethered Ionic Liquid. IP-MCM-PMO. The preparation of IL-PMO with MCM-41 type was carried out by means of a method derived from that reported by Lin et al. for the preparation of MCM-41-type pure silica using ethylamine (EA) as mineralizing agent.[43] CTAB, H_2O, and a mixture of TEOS and **6a** were used as silicic precursor in place of TEOS alone. 2.5 g of CTAB, 100 g of H_2O, and 6.2 mL of EA (70 wt %) were stirred at room temperature. After homogenization of the mixture, 10 mL of TEOS was added dropwise under stirring, and then 3 mmol of **6a** was poured in the reaction mixture. The resulting molar composition of the starting mixture was $1SiO_2$:0.06(**5**):0.15CTAB:1.7EA:$124H_2O$. After being stirred for 4 h at room temperature, the mixture was poured into a polypropylene autoclave that was heated at 100 °C in an oven for 48 h. The slurry was then filtered, washed with ethanol, 500 mL of an ethanol solution of HCl (0.5 N), and then with water. The recovered solid was washed with hot ethanol/HCL in a Soxhlet apparatus, and then dried in air at 80 °C. Yield: 4.13 g.

IP-SBA-PMO. 8.7 g (1.5 mmol) of Pluronic P123 was poured in a HCl (37%) (48.2 g; 0.48 mol) solution in 215 mL of H_2O and stirred at 40 °C for 3 h 30 min, and then 18.53 g (89 mmol) of TEOS was dropwise added to the stirred reaction mixture. After 0.5 h, 3 mmol of **6a** was poured into the reaction mixture. The molar composition of the resulting starting mixture $1SiO_2$: 0.034 (**6a**):0.0168P123:5.4HCl:$134H_2O$ was maintained static at 40 °C for 20 h, and then heated in a Teflon autoclave at 130 °C for 24 h. The slurry was then filtered, and washed with water, ethanol, and ethyl ether. After being washed with refluxing acidified ethanol in a Soxhlet, the solid was dried in air at 80 °C. Yield: 11.47 g.

2.7. Protection of Surfacial Silanol Groups by Trimethylsilation. MCM-41-tms; SBA-15-tms; IP-G-MCM-41-tms; IP-MCM-PMO-tms; IP-G-SBA-15-tms; IP-SBA-PMO-tms. Bis-*O*,*N*-trimethylsilyltrifluoracetamide was used as trimethylsilylating agent for the various solids. The amount of added silane was calculated to be 7 silanes nm^{-2} for calcined SBA-15 and MCM-41 samples and 3.5 silanes nm^{-2} for organic ion-pair-modified mesoporous silicas, respectively. Bis-*O*,*N*-trimethylsilyltrifluoroacetamide was added under argon to each suspension of the grafted silicas (previously activated overnight at 120 °C under vacuum) in toluene (20 mL). The mixture was magnetically stirred for 48 h at 60 °C. The powder was recovered by filtration and successively washed with toluene, methanol, dichloromethane, and diethylether. It was then extracted with dichloroethane/ethylether (1:1) in a Soxhlet apparatus and dried for 2 h in an oven at 80 °C.

Ionic Liquid (IL)-Impregnated SBA-15-tms. To a SBA-15-tms sample (100 mg) previously activated overnight at 120 °C under vacuum was added ionic liquid **6b** (150 mg corresponding to 3 molecules per nm^2 of the solid) in solution in dichloromethane (20 mL). After the mixture was stirred for 3 h, the solvent was gently evaporated, and then the recovered solid was degassed under vacuum.

2.8. Surface Polarity Probing with Reichardt's Dye. The organically functionalized silica samples were dried carefully in vacuum at 120 °C in a Schlenk. After being cooled to room temperature under dried argon, a solution of RD (0.03 μmol of RD per m^2 of solid) in dichloromethane (10 mL) was added to the material. After removal of the solvent under vacuum (10^{-2} Torr) for 2 h, the powder was stored under argon. The diffuse reflectance UV−vis spectrum of the RD-impregnated solid was measured against the corresponding nonimpregnated one.

3. Results and Discussion

3.1. Synthesis of Silylated and Nonsilylated Guanidinium Bis-sulfonimide Ionic Liquids. The cationic guanidinium compounds **3a** and **3b** were synthesized in multistep sequences starting from 1,3-dimethylimidazoline-2-one. Reaction with oxalyl chloride afforded the chloroimidazolinium chloride **1**.[42] This highly reactive intermediate easily reacted with allylamine

Scheme 1. Synthesis of the Nonsilylated Guanidines **2a** and **2b** (Top) and Silylated Guanidine **2a′** (Bottom)

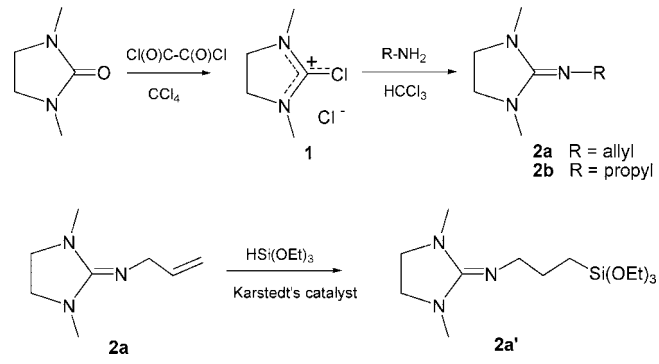

(40) Brunauer, S.; Emmet, P. H.; Teller, E. *J. Am. Chem. Soc.* **1938**, *60*, 309–319.
(41) Broekhoff, J. C. P.; De Boer, J. H. *J. Catal.* **1968**, *10*, 377–390.
(42) Isobe, T.; Ishikawa, T. *J. Org. Chem.* **1999**, *64*, 6984–6988.

Scheme 2. Alkylation of Guanidines

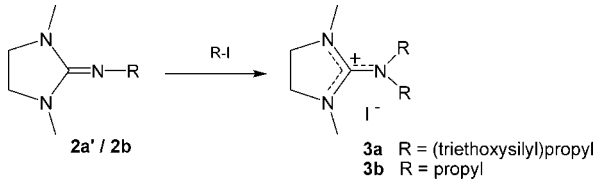

or propylamine to give the corresponding guanidines (**2a/2b**) (Scheme 1, top). Hydrosilylation of the allylguanidine **2a** with triethoxysilane using Karstedt's catalyst led to the triethoxysilylated guanidine (**2a′**) (Scheme 1, bottom).

Alkylation of **2a′** using iodopropyl triethoxysilane gave the bis-silylated guanidinium iodide **3a**, whereas alkylation of **2b** with 1-iodopropane led to the formation of the nonsilylated guanidinium iodide **3b** (Scheme 2).

The ammonium bis-sulfonimides (**5a/5b**) were synthesized in one step by coupling either 2-(4-chlorosulfonylphenyl)ethyltrimethoxysilane (**4a**) or *p*-toluenesulfonyl chloride (**4b**) with trifluoromethanesulfonamide in the presence of an excess of triethylamine (Scheme 3).

Scheme 3. Synthesis of the Silylated Sulfonimide **5a** and the Nonsilylated Sulfonamide **5b**

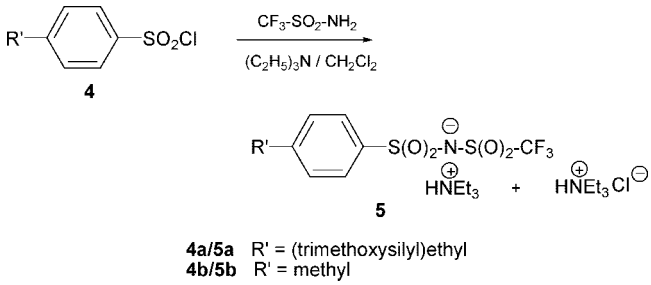

The mixture of the guanidinium iodide (**3a**) and the ammonium bis-sulfonimide (**5a**) in dichloromethane solution gave a suspension (**6a**) containing the tris-silylated guanidinium-sulfonimide ionic liquid, which was identified by electrospray mass spectroscopy after solvent evaporation.

The ionic liquid (**6b**), which is the nonsilylated counterpart of the guanidinium sulfonimide salt (**6a**), was synthesized in a similar manner from nonsilylated precursors **3b** and **5b** as depicted in Scheme 4. After aqueous workup, the obtained compound **6b** was clearly identified by various spectroscopic methods.

Scheme 4. Synthesis of the Trialkoxysilylated IP Precursor **6a** and the Ionic Liquid **6b**

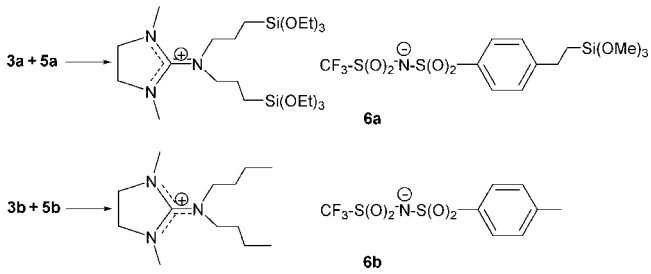

3.2. Preparation of the Organic Ion-Pair-Grafted SBA-15- and MCM-41-type Materials (IP-G-MCM-41/IP-G-SBA-15).

Synthesis and Characterization of MCM-41- and SBA-15-type Pure Silicas. The MCM-41-type pure silica sample[44] was synthesized using pyrogenic silica as silica source and CTAB cationic surfactant as structure-directing agent in basic conditions.[45] The XRD patterns of as-synthesized silica showed an intense peak with a *d* spacing of 42 Å and two weak peaks with lattice *d* spacings of 24 and 21.5 Å, which can be assigned as [100], [110], and [200] reflections associated with the ordered hexagonal (*p6mm*) symmetry because $d_{110} = d_{100}/\sqrt{3}$ and $d_{200} = d_{100}/2$. The corresponding unit cell parameter a_0 was 48 Å. XRD patterns of the calcined MCM-41 revealed a slight silica framework contraction as usually observed, *d* spacing being now 41.3 Å corresponding to a unit cell parameter of 47 Å.

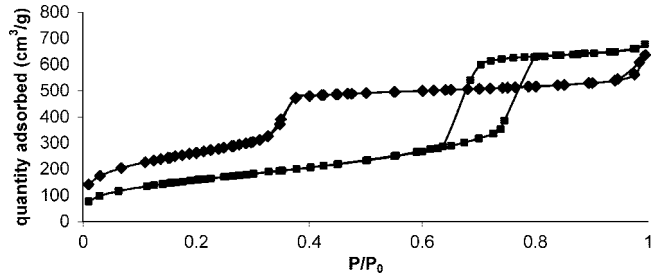

Figure 1. Nitrogen sorption isotherms of materials MCM-41(C) (◆) and SBA-15(C) (■).

Table 1. Textural Characteristics of the Bare Silicas, IP-Grafted Silicas, and IP-PMOs

	XRD		nitrogen sorption isotherms				
sample	d_{100} (Å)	a (Å)	S_{BET} (m^2 g^{-1})	V_{mesop} (mL g^{-1})	V^a_{mesop} (mL g^{-1})	pore diameter (Å)	wall thickness (Å)
MCM-41(C)	41	47	960	0.74	0.74	37	12
IP-G-MCM-41	38	44	(538)	0.23	0.35	22	23
IP-MCM-PMO	51	59	557	0.33[b] 0.75[c]	0.43 0.98	35[b] 180[c]	26
SBA-15(C)	98	113	614	1.0	1.0	89	26
IP-G-SBA-15	96	111	570	0.54	0.87	48	65
IP-SBA-PMO	97	112	586	0.98	1.20	79	37

[a] Pore volume standardized versus pure silica weight. [b] Ascribed to mesopore diameter around 35 Å. [c] Ascribed to mesopore diameter around 180 Å.

The nitrogen sorption isotherm of the sample (Figure 1) featured the characteristic sharp step at 0.35 p/p_0 corresponding to a pore size *D* diameter of 37 Å evaluated by the BdB method, and a mesopore volume of 0.74 mL g^{-1}. The surface area determined by the BET method was 960 m^2 g^{-1}. The wall thickness *e* was calculated using the equation: $e = a_0 - 2r$, where *r* is the apothema of the hexagonal section of the pore having the same section of the cylindrical pore possessing the diameter *D* determined by the nitrogen sorption isotherm using cylindrical pore model and equal to 2.10*r*. Thus, with the equation becoming $e = a_0 - 0.95D$, the calculated *e* value is 12 Å (Table 1).

The SBA-15-type pure silica has been prepared by using a $(EO)_{20}(PO)_{70}(EO)_{20}$ (P123) triblock copolymer and tetraethylorthosilicate in acidic conditions according to a method established in our laboratory,[46] derived from that previously reported by Stucky et al.[47] The heating of the slurry at 130 °C for 24 h

(43) Lin, W.; Cai, Q.; Pang, W.; Yue, Y.; Zou, B. *Microporous Mesoporous Mater.* **1999**, *33*, 187–196.
(44) (a) Kresge, C. T.; Leonowicz, M. E.; Roth, W. J.; Vartuli, J. C.; Beck, J. S. *Nature* **1992**, *359*, 710–712. (b) Beck, J. S.; Vartuli, J. C.; Roth, W. J.; Leonowicz, M. E.; Kresge, C. T.; Schmitt, K. D.; Chu, C. T. W.; Olson, D. H.; Sheppard, E. W. *J. Am. Chem. Soc.* **1992**, *114*, 10834–43.
(45) Galarneau, A.; Desplantier, D.; Dutartre, R.; Di Renzo, F. *Microporous Mesoporous Mater.* **1999**, *27*, 297–308.

was applied to limit the presence of microporosity, which could induce some discrepancy in the surface area and pore volume variations by micropore blockage during subsequent surface functionalization. The XRD of as-synthesized silica showed three well-resolved peaks revealing a highly ordered hexagonal (*p6mm*) pore structure with lattice *d* spacings of 102.6 Å for the [100] peak, 56 Å ([110] peak), and 49 Å for the [200] peak. The corresponding unit cell parameter a_0 derived from the first strong diffraction peak [100] is 118 Å. The calcination brought about slight unit cell contraction in this case too, *d* spacing and unit cell parameter a_0 values becoming 98 and 113 Å, respectively (Table 1).

The nitrogen sorption isotherm of the calcined sample features a characteristic step at 0.71 p/p_0 on the desorption branch of H_1-type hysteresis loop at high pressure, characteristic of large pore mesoporous materials with 1*D* cylindrical channels (Figure 1).The narrow BdB pore size distribution reveals uniform mesopores with a maximum at 89 Å. The materials present a BET surface area of 614 $m^2\ g^{-1}$ and a pore volume of 1.02 mL g^{-1}. The calculated wall thickness *e* of SBA-15 material being of 26 Å is larger than that of the MCM-41 because of the slower rate of the condensation process in acidic media, according to previously reported results about the variation of the wall thickness as a function of the pH of the reaction mixture.[48]

Table 1 gives a survey of the textural characteristics of the parent silicas MCM-41(C) and SBA-15(C) and the ion-pair functionalized materials. It appears that all materials are highly porous solids with specific surface areas in the range from 550 to 960 $m^2 \cdot g^{-1}$. Furthermore, all materials show narrow monodisperse pore size distribution except material IP-MCM-PMO, which shows a bimodal distribution with maximum values at 35 and 180 Å (*vide infra*).

SBA-15 and MCM-41 Silica Surface Grafting with Trisilylated Organic Ion-Pair. Surface modification of both freshly calcined MCM-41- and SBA-15-type silicas with the trisilylated guanidinium−sulfonimide ionic liquid was performed according to a coating method consisting of a sol−gel surface polymerization of the silylated agent as previously tuned up to improve the surface coverage of MCM-41.[49] This method implied the previous physisorption of the silylating agents by contacting the activated siliceous materials with a toluene solution containing 5/3 trialkoxyorganosilane molecules, that is, 5 Si atom per nm^2 of the silica surface, then the addition of a mixture of H_2O:NH_4F:*p*-toluene sulfonic acid (TSA) corresponding to 7.5:0.25:0.25 molecules nm^{-2} of SiO_2, respectively. The amount of added water was adjusted to a 1.5 molar ratio with respect to trialkoxysilyl moieties. This ratio is crucial for hydrolyzing and grafting the alkoxysilane with the nucleophilic assistance of fluorine anion as catalyst. The thermal treatment of the reaction mixture at 60 °C for 6 h under acidic conditions in the presence of *p*-toluene sulfonic acid (TSA) is necessary to achieve the reaction between the silica surface and the organo-ion-pair silane−silanols. The final refluxing step is then considered as final strengthening of the already bonded silane species by more condensation of the silane−silanols to complete total surface coverage.[50] Indeed, besides the use of ammonium fluoride, which favors the trialkoxysilane hydrolysis, the use of acidic media reduces the anarchically vertical polymerization by lowering the silanol condensation rate. The beneficial effect of the use of *p*-toluene sulfonic acid recently received more attention to control the postsynthesis method to graft organic group onto the inside of a SBA-15-type silica.[51]

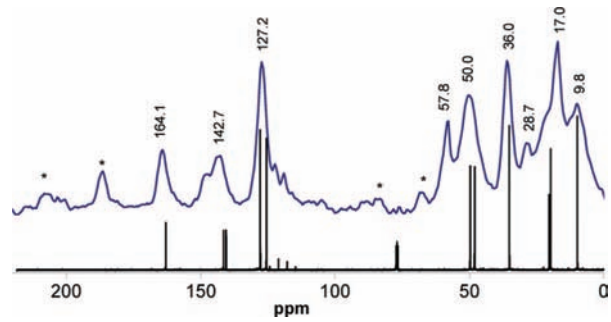

Figure 2. Solid-state CP-MAS NMR spectrum of material IP-G-SBA-15 (top) and liquid ^{13}C NMR spectrum of compound **6b** (bottom); rotational side bands are marked with asterisks.

The obtained materials were characterized by means of ^{29}Si and ^{13}C solid-state NMR spectroscopy. The ^{29}Si one-pulse MAS spectra of the grafted MCM-41 and SBA-15 samples (Supporting Information) show signals located at around −110, −101, and −93 ppm characteristic for Q^4, Q^3, and Q^2 silicon sites of the SiO_4-substructures in the silica framework. Additional peaks observed around −67 and −59 ppm indicate the presence of the T^3 and T^2 sites of the grafted organic moieties.[52] Spectra were modeled using the Dmfit program.[53] The positions obtained for CP-MAS are used to fit the one-pulse data. Integration of the modeled T^n peaks versus Q^n gives valuable information about the surface loading, 1.3 and 1.4 mmol of the grafted ion-pair per gram of pristine silica for MCM-41 and SBA-15, respectively. It is noteworthy that the absence of a peak around −46 ppm characteristic of T^0 sites evidences that all ions are covalently bound to the surface by siloxane bonds.

The chemical shifts observed in the ^{13}C CPMAS spectra of samples IP-G-MCM-41 (Figure 2) and IP-G-SBA-15 as compared to the signal position of neat reagent are consistent with the same chemical structure of the grafted organic moieties, except the signals at $\delta = 9.8$ and 28.7 ppm assigned to the ethylsilane linker $Ar-CH_2-CH_2-SiO_{1.5}$ of the sulfonimide anion. Indeed, the signals at 127.2 and 142.7 ppm together with the shoulder at 148.0 ppm are characteristic of the aromatic carbon nucleus of this anion. However, the large signal at 50 ppm is attributed in part to the two *N*-methyl and two *N*-cyclic carbon atoms of the guanidinium cation in addition to the peak at 164.1 ppm of the quaternary guanidinium carbon atom. Moreover, the signals at 17.0, 36.0, 50.0 ppm are ascribed to the two *N*-propylsilane chains corresponding to the guanidinium cation linkers. The additional peak at 57.8 ppm with the shoulder at 20 ppm was relevant to ethoxysilane groups that were not hydrolyzed or formed during the treatment with HCl/EtOH

(46) Galarneau, A.; Nader, M.; Guenneau, F.; Di Renzo, F.; Gedeon, A. *J. Phys. Chem. C* **2007**, *111*, 8268–8277.
(47) Zhao, D.; Huo, Q.; Feng, J.; Chmelka, B. F.; Stucky, G. D. *J. Am. Chem. Soc.* **1998**, *120*, 6024–6036.
(48) Coustel, N.; Di Renzo, F.; Fajula, F. *J. Chem. Soc., Chem. Commun.* **1994**, 967–968.
(49) (a) Abramson, S.; Laspéras, M.; Galarneau, A.; Desplantier-Giscard, D.; Brunel, D. *Chem. Commun.* **2000**, 1773–1774. (b) Martin, T.; Galarneau, A.; Brunel, D.; Izard, V.; Hulea, V.; Blanc, A. C.; Abramson, S.; Di Renzo, F.; Fajula, F. *Stud. Surf. Sci. Catal.* **2001**, *135*, 4621–4628.
(50) Martin, T.; Lefevre, B.; Brunel, D.; Galarneau, A.; Di Renzo, F.; Fajula, F.; Gobin, P. F.; Quinson, J. F.; Vigier, G. *Chem. Commun.* **2002**, 24–25.
(51) (a) García, N.; Benito, E.; Guzmán, J.; Tiemblo, P.; Morales, V.; García, R. A. *Microporous Mesoporous Mater.* **2007**, *106*, 129–139. (b) García, N.; Benito, E.; Guzmán, J.; Tiemblo, P. *J. Am. Chem. Soc.* **2008**, *129*, 5052–5060.

Table 2. Chemical Composition of IP-Grafted Mesostructured Silicas and IP-PMOs

sample	ion-pair loading (mmol g^{-1} SiO_2) elemental analyses	ATG[a]	NMR ^{29}Si MAS	elemental composition from elemental analysis
IP-G-MCM-41	1.10	1.12(1.26)	1.19	$Si_{15.2}C_{22.1}N_{4.0}S_{1.7}F_3$
IP-MCM-PMO	0.51	0.66(0.81)	0.72	$Si_{32.5}C_{28.9}N_{4.24}S_{1.97}F_3$
IP-G-SBA-15	1.14	1.35(1.43)	1.27	$Si_{14.6}C_{23.5}N_{4.4}S_{2.06}F_3$
IP-SBA-PMO	0.33	0.51(0.51)	0.47	$Si_{51.2}C_{29.4}N_{3.9}S_{2.2}F_3$

[a] In parentheses: values obtained by TG-DSC measurements.

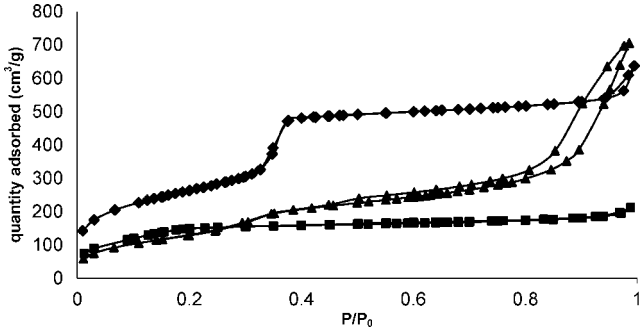

Figure 3. Nitrogen sorption isotherms of materials MCM-41 (C) (◆), IP-G-MCM-41(■), and IP-MCM-PMO (▲).

solution particularly for the surfactant removal from the as-synthesized PMOs materials.[35,54]

FTIR spectra of the grafted materials IP-G-MCM-41 and IP-G-SBA-15 confirm the structure of the attached guanidinium−sulfonimide ion-pair entities. The prominent features of the IR spectra are four C−H stretching bands below 3000 cm^{-1} and C−N deformation bands at 1609 and 1568 cm^{-1}.

The elemental composition of the hybrid materials IP-G-MCM-41 and IP-G-SBA-15 has been determined by elemental analyses, thermogravimetry, and ^{29}Si MAS NMR spectroscopy. The data are reported in Table 2. The elemental analyses of the materials are given in the Supporting Information.

Taking into account the chemical formula of the guanidinium−sulfonimide ion-pair (IP) attached to the silica surface, the relative experimental value of each heteroelement of the organic moieties (H_i), where i corresponds to the heteroelement number in the formula, is in good agreement with the theoretical value. Nevertheless, the carbon value is over estimated, what can be attributed to incomplete hydrolysis and condensation of the alkoxysilane.

The ion-pair mole number n_{IP} per gram of pure silica was calculated using the general formula (1):

$$n_{IP} = (h\% \times M_{Si})/(Si\% \times M_{SiO2}) \quad (1)$$

where $h\%$ corresponds to $\sum Hi\%/(nM_{Hi})/i$, and M_{Si} and M_{SiO2} are the atom mass of silicon and the molar mass of silica, respectively (for further information, see Supporting Information).

When the organic grafting was estimated from TGA measurements instead of elemental analysis, decomposed weight/residual (SiO_2) weight at 700 °C stems from grafted organically amounts on silica corresponding to amount based on 1 g of silica.

The formula (2) used for the calculation of n_N from the TGA data was as follows:

$$n_{IP} = \text{org wt \}/[100 - (\text{org wt \} - H_2O \text{ wt \})] \times (M_{IP} - 3M_{H_2O}) \quad (2)$$

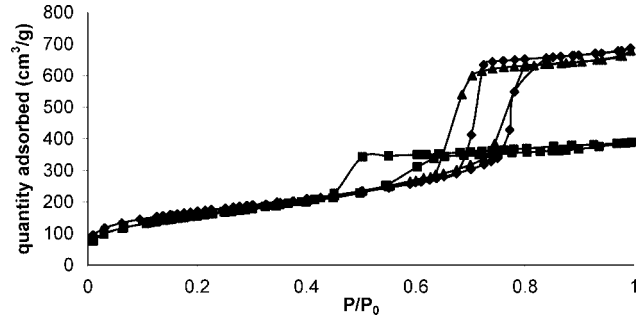

Figure 4. Nitrogen sorption isotherms of materials SBA-15 (C) (◆), IP-G-SBA-15 (■), and IP-SBA-PMO (▲).

where org wt % was the weight fraction of the organic part per SiO_2 ($M_{IP} - M_{H2O}$) representing the water lost per grafted molecule, taking into account the formation of one silanol function following one Si−C bond oxidation. The two sets of data show a relative agreement even though the discrepancy between them is noticeable in the case of IP-G-SBA-15.

The three sets of data represented in Table 2 show a good agreement of the n_{IP} values of the different materials obtained from elemental analysis, ^{29}Si MAS NMR spectroscopy, and thermogravimetry. The higher n_{IP} values obtained from ATG can be explained by slightly higher carbon content of the materials resulting from etherification of silanol groups under acidic conditions during Soxhlet extraction necessary for total surfactant removal.[35,54] This is confirmed by exalted carbon values in the microanalyses of the materials and characteristic signal for ethoxysilyl groups in the ^{13}C CP-MAS NMR spectra of the materials IP-MCM-PMO and IP-SBA-PMO. Furthermore, the elemental analyses data give detailed information concerning the exact elemental composition of the materials. The ratios between the three heteroelements N, S, and F are near to the expected values of the triethoxysilylated precursor **6a**. As the nitrogen value is characteristic for the quantity of immobilized guanidinium cations and sulphur and fluorine are representative for the sulfonimide anion, this result confirms equimolar quantities of the immobilized guanidinium and sulfonimide species and excludes the presence of noticeable amounts of other salts e.g. triethylammonium halides.

The nitrogen sorption isotherms of the samples before and after functionalization shown in Figures 3 and 4 reveal that the mesoporous nature of the materials is preserved even though the grafting has occurred. The textural parameters of the samples before and after surface functionalization were summarized in Table 1.

It is noteworthy that the variations of the surface area, total pore volume, and pore diameter of the IP-grafted samples are lower than the corresponding values for the parent materials as a consequence of the organic coverage. Moreover, the decrease in the pore volume standardized versus pure silica weight assesses that the lining is happening inside the mesopores, which decreases also the pore diameter size as shown by the steep adsorption step shift to low pressure. As expected, the relative decrease in the pore size of MCM-41 is more important than that observed with the parent SBA-15, and the material becomes nearly supermicroporous. Functionalized IP-G-MCM-41 and IP-G-SBA-15 still show XRD patterns similar to those of the parent materials MCM-41(C) and SBA-15(C). These results confirm

(52) Wiench, J. W.; Avadhut, Y. S.; Maity, N.; Bhaduri, S.; Kumar Lahiri, G.; Pruski, M.; Ganapathy, S. *J. Phys. Chem. B* **2007**, *111*, 3877–3885.

that the initial texture is preserved during the grafting reaction. However, the decrease in diffraction intensity of the [100] reflection and the absence of the [110] and [200] reflections in the case of MCM-41 indicate that the structural order of these materials did not show long-range order, which is usually observed during modification of this type of mesoporous materials.[55]

The TEM pictures of the grafted silicas MCM-41 and IP-G-SBA-15 (see Supporting Information) also reveal the preservation of the mesoporous system during the coating process.

3.3. Synthesis and Characterization of the Organic Ion-Pair-Tethered MCM-41 and SBA-15 PMOs (IP-MCM-PMO/IP-SBA-PMO). The synthesis of ordered surfactant-templated periodic mesoporous organosilicas (PMOs) with bridging organic groups in the framework has been first carried out by using bis-silylated precursors in the presence of surfactant.[32,55,56] In the case of the exclusive use of organosilane as the only silicon source, a well-structured PMO framework can be formed provided that the organic moieties of the organosilane do not contain complex functionality or large number of carbon. In the case of more complex organosilane, well-structured PMO formation requires the addition of variable amounts (typically from 50 to 95 wt %) of tetraalkoxysilane as co-condensing agent, to permit some relaxation of the hybrid framework.[57] Such a strategy was adopted in this work.

The synthesis of IP-PMO featuring MCM-41-type architecture (IP-MCM-PMO) was performed using cetylammonium bromide as structure-directing agent under basic conditions using diethylamine (EA) as mineralizing agent, according to the method to prepare bare MCM-41-type silica with TEOS.[58] This methodology has been further adapted to prepare PMOs incorporating tartrate derivatives in the silica framework using bis-silylated tartramide with the range tartramide to TEOS from 0.05 to 0.13 corresponding to a ratio alkoxysilyl group:TEOS of 0.26:1 in the highest organosilane loading.[59] In our case, the solid containing ion-pair was prepared according to the same reaction mixture composition as in previous works except for the use of tris-silylated ion-pair in place of bis-silylated tartramide ligand, with a silylated ion-pair:TEOS ratio of 0.06:1, which corresponds to a alkoxysilane group:TEOS ratio of 0.18:1. Finally, the composition of the reaction mixture was $1SiO_2$:0.13CTAB:1.44EA:$105H_2O$, the composition of the silica source being $(RO)_3$Si-IP:TEOS = 0.18:1 with the successive addition of TEOS and the silylated ion-pair to the CTAB/EA solution.

The synthesis method of PMO featuring SBA-15 (material IP-SBA-PMO) was derived from those already reported for the preparation of highly ordered large-pore periodic mesoporous organosilica having the SBA-15 structure using nonionic triblock copolymer Pluronic P123 as the template under acidic conditions with the aid of inorganic salts.[35] The silylated ion-pair:TEOS ratio was chosen from the ones giving the best structurating effect observed during the direct synthesis of ordered SBA-15 mesoporous materials containing arenesulfonic acid.[60,61] As the SBA-15 wall thickness is larger than that of MCM-41-type silica, a lower silylated IP:TEOS ratio was used than for the synthesis of the IP-MCM-PMO material, that is, a 0.033:1 ratio, corresponding to a alkoxysilane:TEOS ratio of 0.1:1. As the rate of gelification in acidic media is lower than that in basic ones, the silylated ion-pair was added one-half an hour after the TEOS addition to the warm Pluronic P123 acid solution. In this case, the composition of the reaction mixture corresponded to $1SiO_2$:0.0152P123:4.9HCl:$122H_2O$.

The characterization of the obtained materials gave insight in their structure and surface properties. The ^{13}C CPMAS spectra of both IP-MCM-PMO and IP-SBA-PMO feature the same pattern as that already observed in the case of the grafted materials. However, no carbon signal due to CTAB or P123 was observed, demonstrating the total removal of the surfactants using refluxing acidic ethanol extraction. The FTIR spectra of the materials show also the same bands as compared to the samples functionalized with tethered IP, thus confirming the preservation of the ion-pair moieties during the synthesis procedure of PMO, under both basic and strongly acidic conditions.

It is noteworthy that the ^{29}Si MAS NMR spectrum of the PMO silicas reveals a higher Q^3/Q^4 ratio but a lower T^2/T^3 ratio than those of the grafted silicas (Supporting Information). Indeed, the grafted materials, resulting from the pure calcined silicas, retained the high condensation degree of their framework demonstrated by a lower Q^3/Q^4 ratio than that of PMOs, prepared by one-pot synthesis. In the latter case, less silanol condensation occurred due to the absence of high temperature treatment. On the contrary, the relatively strong intensity of the T^3 signals in the case of the PMO-type materials is consistent with a high degree of silane−silanol condensation during the one-pot synthesis wathever the pH conditions. In the case of the materials obtained by grafting, silane−silanol condensation during the surface coating was restrained for sterical reasons. Actually, three Si−O−Si linkages from the tetrahedral silane−silicon atom with at least one surface silanol and neighbor silane−silanols is difficult to achieve. In contrast, concerning PMO materials obtained by one-pot syntheses, the silane silicon atom is inherent in part of the silica wall, hence featuring nearly the same condensation degree as compared to the siliceous framework.

The chemical composition of the PMO summarized in Table 2 reveals a lower IP loading than that into the corresponding grafted mesostructured silicas.

We have suspected the critical importance of the use of tris-silylated organic ion-pair in addition with TEOS, taking into account the role of salt addition during the structuring of mesoporous pure silicas with either MCM-41[62−64] or SBA-15 structure.[35]

The nitrogen sorption isotherms of IP-MCM-PMO (Figure 3) and IP-SBA-PMO (Figure 4) reveal totally different structuring effects. In the case of the IP-MCM-PMO, the isotherm

(53) Massiot, D.; Fayon, F.; Capron, M.; King, I.; Le Calvé, S.; Alonso, B.; Durand, J.-O.; Bujoli, B.; Gan, Z.; Hoatson, G. *Magn. Reson. Chem.* **2002**, *40*, 70–76.
(54) (a) Guan, S.; Inagaki, S.; Ohsuna, T.; Terasaki, O. *Microporous Mesoporous Mater.* **2001**, *44−45*, 165–172. (b) Kapoor, M. P.; Inagaki, S. *Chem. Mater.* **2002**, *14*, 3509–3514.
(55) Zheng, S.; Gao, L.; Guo, J. *Mater. Chem. Phys.* **2001**, *71*, 174–178.
(56) Kuroki, M.; Asefa, T.; Whitnal, W.; Kruk, M.; Yoshina-Ishii, C.; Jaroniec, M.; Ozin, G. A. *J. Am. Chem. Soc.* **2002**, *124*, 13886–13895.
(57) (a) Asefa, T.; MacLachlan, M. J.; Coombs, N.; Ozin, G. A. *Nature* **1999**, *402*, 867–871. (b) Asefa, T.; MacLachlan, M. J.; Grondey, H.; Coombs, N.; Ozin, G. A. *Angew. Chem., Int. Ed.* **2000**, *39*, 1808–1811.
(58) Lin, W.; Cai, Q.; Pang, W.; Yue, Y.; Zou, B. *Microporous Mesoporous Mater.* **2000**, *33*, 187–196.
(59) García, R. A.; van Grieken, R.; Iglesias, J.; Morales, V.; Gordillo, D. *Chem. Mater.* **2008**, *20*, 2964–2971.
(60) Melero, J. A.; Stucky, G. D.; van Grieken, R.; Morales, M. *J. Mater. Chem.* **2002**, *12*, 1664–1670.
(61) Wang, X.; Chen, C.-C.; Chen, S.-Y.; Mou, Y.; Cheng, S. *Appl. Catal., A* **2005**, *281*, 47–54.
(62) Yu, J.; Shi, J.-L.; Chen, H.-R.; Yan, J.-N.; Yan, D.-S. *Microporous Mesoporous Mater.* **2001**, *46*, 153–162.

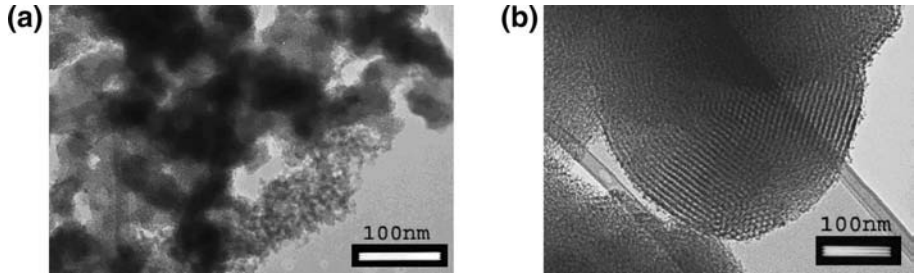

Figure 5. (a,b) TEM micrographs of materials IP-MCM-PMO (left) and IP-SBA-PMO (right).

features a smooth step at a relative pressure p/p_0 around 0.32 corresponding to a pore size of approximately 35 Å and an additional H4 hysteresis loop at relatively high pressure, which indicates the presence of a large amount of secondary large mesopores of a diameter of approx 180 Å (Table 1). Following these results, the first adsorption step would correspond to a three-dimensional disordered network of short "wormlike" mesopore channels similar to the primary mesopore structure of MCM-41 synthesized in the presence of additional salts.[64] Most of the mesoporous silicas prepared in the presence of additional NaCl exhibit an additional H4-type hysteresis loop at high p/p_0 values indicating the presence of a secondary mesopore system similar to a KIT-1 structure.[62,64] This morphology could be related to the second adsorption step at a relative pressure of $p/p_0 \approx 0.9$. The XRD pattern (Supporting Information) confirms the lower degree of long-range ordering, also demonstrated by the absence of additional higher order peaks, which is characteristic of well-formed hexagonal pore arrays. A variation of the structuring effect induced by the presence of salt has been already reported during the synthesis of bare MCM-41 in the presence of tetrapropylammonium (TPA^+) cation as a function of the salt concentration. At low concentration of TPA^+ in the sol, an increase in TPA^+/surfactant ratio up to 2.0 induced an increase of long-range ordering. In contrast, at high salt concentration (TPA^+/surfactant > 2.0), an additional increase in the cationic TPA^+ concentration led to lower ordering and gave poorly crystalline or amorphous materials.[63] In the case of IP-MCM-PMO, it appeared that during the formation of the surfactant−silicate mesostructure, the electrostatic interaction between the cationic surfactant and the silicate anions was altered by the presence of the additional salt of the silylated ion-pair, leading to a lower charge density at the surfactant inorganic interface, which controls the assembly process. However, the effective headgroup area of the surfactant increased and the transition of the surfactant mesophase occurred from hexagonal MCM-41 to disorded KIT-1.[62,64]

Interestingly, in the case of the IP-SBA-PMO, the pattern of the nitrogen sorption isotherm is very similar to that of the calcined pure SBA-15 silica. Indeed, this isotherm reveals a very sharp increase in the nitrogen uptake at p/p_0 of 0.76 for adsorption and desorption at p/p_0 of 0.67, indicating a relative uniform pore size distribution around 79 Å according to the BdB treatment of the desorption branch (Figure 4). The powder X-ray diffractogram of this sample (Supporting Information) reveals the presence of the [110] and [200] reflections besides the [100] reflection, revealing a highly ordered hexagonal (*p6mm*) pore structure with lattice *d* spacings of 97 Å ([100] reflection), 56 Å ([110] reflection), and 49 Å ([200] reflection). The corresponding unit cell parameter a_0 derived from the first strong diffraction peak [100] is 112 Å.

Scanning electron microscopy of the IP-G-SBA-15 material shows rodlike particles of 1–2 μm thickness similar to the morphology of SBA-15 type materials described in the literature.[65] In the case of the IP-SBA-PMO the rodlike units appear more elongated as already mentioned as a result of the presence of ionic species. In contrast, the morphology of the IP-G-MCM-41 material indicates the formation of monodispersed primary spherical particles of ~0.1 μm diameter, whereas the IP-MCM-PMO features a much bigger and polydisperse particle size of 1−5 μm (see Supporting Information).

Transmission electron micrographs of both IP-MCM-PMO and IP-SBA-PMO (Figure 5a and b) clearly unveil the difference between the architecture of the two mesoporous materials. The IP-MCM-PMO image reveals different kinds of texture with structural defects and disordered channel arrangements, which are consistent with the texture deduced from the nitrogen sorption isotherm analysis. The micrograph of the IP-SBA-PMO material provides a direct visualization of well-ordered hexagonal arrays of 1D mesoporous channels particularly along the direction of the pore axis or in the direction perpendicular to the pore axis. This result is in good agreement with the conclusion withdrawn from the N_2 sorption measurement and confirms the beneficial effect of the salt addition brought by the use of silylated ionic liquid precursor on the structuration in the case of the IP-SBA-PMO materials in contrast with that observed in the case of IP-MCM-PMO.[35] Anyway, it was also reported that several typical nonionic surfactants aggregated into micelles in 1-ethyl-3-methylimidazolium bis(trifluoromethylsulfonyl)imide), while no aggregation was observed with cetyltrimethylammonium bromide.[66] That suggests that the presence of silylated ionic liquid favors the assembly between the headgroups of triblock copolymer surfactant and the protonated silanols species. This interaction may lead to the formation of highly ordered large-pore PMO materials according to a $(S^0H^+)(X^-I^+)$ pathway, while the micellar aggregation of CTAB would be stamped out in the presence of ionic liquid.

At this stage, mesoporous materials bearing covalently attached guanidinium sulfonimide ion-pairs can be prepared either by the grafting the nanostructured silica surface with silylated ionic precursors or by incorporating organic ion-pair moieties into the materials' framework during a one-pot sol−gel synthesis. In the first case, the texture of the bare mesoporous silica is preserved. For the IP-G-MCM-41, grafting led to a strongly decreased pore size (<25 Å), giving a material with supermicroporosity, whereas the IP-G-SBA-15 always featured a mesoporous system. In the second case, the IP-MCM-PMO prepared with CTAB as template in basic conditions shows a very disordered structure. In contrast, the IP-PMOs prepared with P123 in acidic conditions (IP-SBA-PMO) feature a very well-ordered architecture on a mesoscopic length scale possessing larger pore size, even as compared to grafted material IP-G-SBA-15.

(63) Das, D.; Tsai, C.-M.; Cheng, S. *Chem. Commun.* **1999**, 473–474.

Scheme 5. Structure of the Ground State and First Excited State of RD

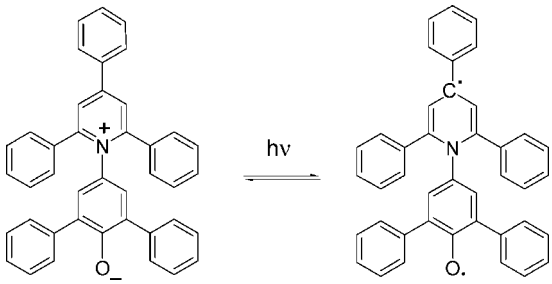

3.4. Solvatochromic Determination of the Surface Polarity. In order to get more information about the resulting polarity of the ion-paired modified solids, the surface properties of the various materials were investigated by solvatochromism. Reichardt's dye (RD) is one of the most common negative solvatochromic charge-transfer (CT) absorption probes to empirically measure the polarity of homogeneous media by means of the $E_T(30)$ parameter value, defined as the molar electronic transition energy (eq 3):

$$E_T(30)\ (\text{kcal mol}^{-1}) = 28\,591/\lambda_{max}\ (\text{nm}) \qquad (3)$$

where λ_{max} is the maximum of the longest intramolecular charge-transfer $\pi-\pi^*$ absorption wavelength of the zwitterionic 2,6-diphenyl-4-(2,4,6-triphenyl-*N*-pyridino)phenolate molecule in solution.[37] The λ_{max} is very medium dependent as shown by the solvatochromic shifts of RD featuring a high sensitivity due to the largest dipole moment change of the ground sate as compared to the lowest excited one (Scheme 5).

The higher stabilization of the ground state is due to the larger dipole moment of the zwitterionic form, leading to an increase of the transition energy featured by a shifting of E_T values in going from $E_T^{(water)} = 63.1$ for water to $E_T^{(TMS)} = 32.4$ for tetramethylsilane.[67,68]

The dimensionless normalized E_T^N scale was defined according to eq 4 using water and tetramethylsilane as extreme polar and nonpolar solvents.

$$E_T^N = [E_T^{(solvent)} - E_T^{(TMS)}]/[E_T^{(water)} - E_T^{(TMS)}] = [E_T^{(30)} - 30.7]/32.4 \qquad (4)$$

This scale was also used to check the surface polarity of mineral oxides such as silica[38,69] and organically modified functionalized silicas,[70−72] considering $E_T^{(solid)}$ in place of $E_T^{(solvent)}$.

The range of $E_T(30)$ of silica surface (naked and organically modified) depending on its surface coverage is going from 0.77 (calcined silica) to 0.45 ($O_{1.5}Si(CH_2)_3NH_2$/HMDS) corresponding to 3-propylaminosilylated silica subsequently passivated with hexamethyldisilazane.[73]

Table 3. E_T^N Values for Passivated IP-PMOs and IP-Grafted Silicas versus Passivated Mesostructured Silicas

entry	sample	λ_{max}	$E_T^{(30)}$	E_T^N	ΔE_T^{Na}
1	MCM-41[b]	525	54.45	0.73	0.34
2	MCM-41-tms	660	43.32	0.39	0
3	SBA-15[b]	525	54.45	0.73	0.32
4	SBA-15-tms	650	43.99	0.41	0
5	IL-impregnated SBA-15-tms	539	53.04	0.69	0.28
6	IP-G-MCM-41-tms	625	45.74	0.465	0.075
7	IP-MCM-PMO-tms	600	47.65	0.52	0.13
8	IP-G SBA-15-tms	575	49.72	0.59	0.18
9	IP-SBA-PMO-tms	600	47.65	0.52	0.11

[a] Versus parent tms-passivated silica. [b] Pure mesostructured silica.

Table 3 lists the λ_{max} of the CT band of the various materials and the corresponding E_T^N values for each material in addition to the ionic liquid physisorbed on passivated SBA-15-tms (entry 5, IL-impregnated SBA-15-tms).

To probe the accessibility of the RD probe to the immobilized ionic pair of the different IP-containing materials, we first considered the polarity difference ΔE_T^N between nonpassivated and tms-passivated silicas (entries 1−4). Considering the passivated materials MCM-41-tms and SBA-15-tms as the most apolar references (entries 2 and 4), the polarity increment associated with the presence of surface silanol groups of nonpassivated silicas corresponds to 0.34 and 0.32 for MCM-41 and SBA-15 structure, respectively (entries 1 and 3). Interestingly, the polarity increment of the IL-impregnated SBA-15-tms sample of 0.28 (entry 5) is just slightly lower than the pure silicas, hence featuring a very polar surface in accordance with the unexpected high solvatochromic polarity of most ionic liquids reported in the literature.[33] In a second time, we investigated the polarity increments associated with the ion-pair-containing materials (entries 6−9). Except for the IP-G-MCM-41-tms, the IP-functionalized materials show significantly enhanced polarity as compared to the related passivated silicas (entries 7−9). The highest value ($\Delta E_T^N = 0.18$) was observed for the IP-G-SBA-15-tms material (entry 8). Slightly lower values ($\Delta E_T^N = 0.13/0.11$) were observed for the materials obtained by one-pot procedures (IP-MCM-PMO-tms/entry 7 and IP-SBA-PMO-tms/entry 9). This slight difference may be due to a lower IP-loading as indicated by elemental analysis, ATG measurements, and solid-state NMR spectroscopy (Table 2). However, the values for the PMO type materials confirm ion-pair−RD interaction and location of the guanidinium-sulfonimides on the pore surface similarly to the material IP-G-SBA-15.

In contrast, a lower ΔE_T^N value ($\Delta E_T^N = 0.075$) was observed with the IP-G-MCM-41-tms (entry 6). This lower value would result from the lower diffusion of the RD probe inside the porous volume due to the small pore size as compared to the kinetic diameter of the RD molecule (∼15 Å), giving interactions only with ion-pairs located at the outer particle surface. This assumption is also based on a different surface potential of the outer surface of the particles as compared to the inner pore surface of the mesostructured pure silica. Even with high ion-

(64) (a) Ryoo, R.; Kim, J. M.; Chin, C. H. *J. Phys. Chem.* **1996**, *100*, 17718–17721. (b) Kim, J. M.; Jun, S.; Ryoo, R. *J. Phys. Chem. B* **1999**, *103*, 6200–6205.
(65) Yu, C.; Fan, J.; Tian, B.; Zhao, D. *Chem. Mater.* **2004**, *16*, 889–898.
(66) Fletcher, K. A.; Pandey, S. *Langmuir* **2004**, *20*, 33–36.
(67) Chastrette, M.; Carretto, J. *Can. J. Chem.* **1985**, *63*, 3492–3498.
(68) Reichardt, C. *Solvents and Solvent Effects in Organic Chemistry*, 3rd ed.; Wiley-VCH: Weinheim, Germany, 2003; Table 7-3, pp 418−424.
(69) Rottman, C.; Grader, G. S.; Hazan, Y. D.; Avnir, D. *Langmuir* **1996**, *12*, 5505–5508.
(70) (a) Spange, S.; Reuter, A. *Langmuir* **1990**, *15*, 141–150. (b) Spange, S.; Reuter, A.; Lubda, D. *Langmuir* **1990**, *15*, 2103–2111.
(71) Taverner, S. J.; Clark, J. H.; Gray, G. W.; Heath, P. A.; Macquarrie, D. *Chem. Commun.* **1997**, 1147–1148.
(72) Fiorilli, S.; Onida, B.; Macquarrie, D. J.; Garrone, E. *Sens. Actuators, B: Chem.* **2004**, *B100*, 103–106.
(73) Macquarrie, D. J.; Taverner, S. J.; Stewart, J.; Gray, G. W.; Heath, P. A.; Rafelt, J. S.; Saulzet, S. I.; Hardy, J. J. E.; Clark, J. H.; Sutra, P.; Brunel, D.; di Renzo, F.; Fajula, F. *New J. Chem.* **1999**, *23*, 725–731.

pair loading comparable to that of the IP-SBA-PMO-tms, this material shows a reduced amount of accessible ionic species.

The opposite trends of the ETN values of the IP-MCM- and the IP-PMO-type materials can therefore be explained by different morphological features of the solids on a mesoscopic length scale. However, these results reveal good accessibility of the anchored ion-pairs in the case of the PMO type and grafted IP-G-SBA-15-tms materials. This result evidences the IP location at the whole pore surface. Such a fact would result from the location of the silylated IP precursor molecules at the interface between the positively charged headgroup of the surfactant and the inorganic species during hydrolysis−polycondensation in the case of the PMO type materials. Interestingly, in the case of IP-PMOs as well as for the IP-grafted materials, homogeneous location of the ion-pairs inside the pore channels suggests a monophasic nature of the PMO materials.

4. Conclusion

We report the synthesis of new guanidinium−sulfonimide ionic liquids. A trisilylated ionic liquid based on a disilylated guanidinium and a monosilylated sulfonimide ion-pair was synthesized and compared to its nonsilylated ionic liquid counterpart prepared in parallel. The trisilylated guanidinium−sulfonimide ionic liquid allowed one to achieve the successful preparation of periodic mesoporous organosilica containing an attached ion-pair, which was covalently anchored on silica surface by both the organo-cationic and the organo-anionic moieties. This kind of material has never been reported up to now.

We focused on the synthesis of ion-pair-containing materials by two strategies. For the first time, mesostructured silica frameworks possessing MCM-41-type and SBA-15-type structures were grafted with the silylated guanidinium−sulfonimide ionic liquid to give hybrid mesoporous "organo-ionic"−inorganic materials. These materials were compared to related PMO materials, prepared by the one-pot sol−gel procedure of the silylated guanidinium−sulfonimide ion-pair with tetraethoxysilane. Characterization of the latter materials by solid-state NMR and elemental analysis indicated that the anchored ion-pairs were preserved in the materials, despite the drastic synthesis conditions in terms of strongly basic strength of the reaction mixture using CTAB as surfactants or strongly acid using P123. The use of trisilylated ion-pair in addition with tetraethoxysilane did not provide a beneficial effect on the structuration of PMO material possessing the MCM-type structure, while the SBA-15-type PMO containing the guanidinium−sulfonimide ion-pair showed an excellent mesostructure due to a specific salt effect. Finally, the polarity of the surface of the set of materials was determined using Reichardt's dye (RD) as a probe. This study revealed the presence of the organoion-pair located on the pore surface whatever the preparation type of the materials, thus suggesting the monophasic nature of the IP-PMO materials.

Acknowledgment. A.E.K. is grateful to the Institut Carnot for funding. P.H. thanks the "Groupement de Recherche PARIS" and the "Reseau de Recherche 3, Chimie pour le Développement Durable" of the CNRS for financial support. We are indebted to Thomas Cacciaguerra, Géraldine Layrac, and Eva Rettenmeier for technical assistance with HRTEM images and XRD measurements and to the Service Central d'Analyse (CNRS, Solaize, France), particularly to Jean-Louis Imbert, for his help.

Supporting Information Available: Experimental details for the synthesis of MCM-41 and SBA-15 type silicas, elemental analysis, ^{29}Si MAS, ^{13}C CP-MAS NMR and FT-IR spectra, X-ray diffractograms, TG-DSC plots, and TEM/SEM images of the ion-pair functionalized materials; BJH desorption plot of material IP-MCM-PMO. This material is available free of charge via the Internet at http://pubs.acs.org.

JA807630J